Rapid, electronically controllable transverse mode selection in a multimode fiber laser

J. M. O. Daniel* **and W. A. Clarkson**

Optoelectronics Research Centre, University of Southampton, UK
*J.Daniel@soton.ac.uk

Abstract: A novel technique for the electronically-controllable generation and switching of transverse modes within a multi-mode fiber laser oscillator is presented. Preliminary results demonstrate individual transverse mode lasing and fast switching between modes with watt-level output powers. When applied to a core-pumped Tm-doped silica fiber laser with a multimode core the fundamental mode (LP_{01}), the next higher order mode (LP_{11}), or a donut-shaped LP_{11} superposition were selectively excited with power levels in excess of 5 W. Fast switching between LP_{01} and LP_{11} modes at up to 20kHz was also realized.

OCIS codes: (140.3510) Lasers, fiber; (140.3295) Laser beam characterization.

References and links

1. D. J. Richardson, J. Nilsson, and W. A. Clarkson, "High power fiber lasers: current status and future perspectives [Invited]," J. Opt. Soc. Am. B **27**(11), B63 (2010).
2. J. M. Fini and J. W. Nicholson, "Bend compensated large-mode-area fibers: achieving robust single-modedness with transformation optics," Opt. Express **21**(16), 19173–19179 (2013).
3. J. Limpert, F. Stutzki, F. Jansen, H.-J. Otto, T. Eidam, C. Jauregui, and A. Tünnermann, "Yb-doped large-pitch fibres: effective single-mode operation based on higher-order mode delocalisation," Light Sci. Appl. **1**(4), e8 (2012).
4. J. P. Koplow, D. A. V. Kliner, and L. Goldberg, "Single-mode operation of a coiled multimode fiber amplifier," Opt. Lett. **25**(7), 442–444 (2000).
5. J. C. Knight, T. Birks, R. F. Cregan, P. S. J. Russell, and J.-P. de Sandro, "Large mode area photonic crystal fibre," Electron. Lett. **34**(13), 1347 (1998).
6. S. Ramachandran, J. M. Fini, M. Mermelstein, J. W. Nicholson, S. Ghalmi, and M. F. Yan, "Ultra-large effective-area, higher-order mode fibers: a new strategy for high-power lasers," Laser Photon. Rev. **2**(6), 429–448 (2008).
7. J. M. Fini and S. Ramachandran, "Natural bend-distortion immunity of higher-order-mode large-mode-area fibers," Opt. Lett. **32**(7), 748–750 (2007).
8. V. Niziev and A. Nesterov, "Influence of beam polarization on laser cutting efficiency," J. Phys. D Appl. Phys. **32**(13), 1455–1461 (1999).
9. M. Meier, V. Romano, and T. Feurer, "Material processing with pulsed radially and azimuthally polarized laser radiation," Appl. Phys., A Mater. Sci. Process. **86**(3), 329–334 (2007).
10. M. Duocastella and C. B. Arnold, "Bessel and annular beams for materials processing," Laser Photon. Rev. **6**(5), 607–621 (2012).
11. N. Sanner, N. Huot, E. Audouard, C. Larat, and J.-P. Huignard, "Direct ultrafast laser micro-structuring of materials using programmable beam shaping," Opt. Lasers Eng. **45**(6), 737–741 (2007).
12. J. M. O. Daniel, J. S. P. Chan, J. W. Kim, J. K. Sahu, M. Ibsen, and W. A. Clarkson, "Novel technique for mode selection in a multimode fiber laser," Opt. Express **19**(13), 12434–12439 (2011).
13. F. Havermeyer, W. Liu, C. Moser, D. Psaltis, and G. J. Steckman, "Volume holographic grating-based continuously tunable optical filter," Opt. Eng. **43**(9), 2017 (2004).
14. T. Mizunami, T. V. Djambova, T. Niiho, and S. Gupta, "Bragg gratings in multimode and few-mode optical fibers," J. Lightwave Technol. **18**(2), 230–235 (2000).
15. A. W. Snyder and W. R. Young, "Modes of optical waveguides," J. Opt. Soc. Am. **68**(3), 297 (1978).

1. Introduction

Scaling core area in a fiber laser, whilst preserving the ability to select a single transverse mode (usually the fundamental mode), is a topic which continues to attract much interest within the laser community [1–3]. The need for larger mode areas to mitigate against damage

#196993 - $15.00 USD Received 10 Sep 2013; revised 2 Nov 2013; accepted 5 Nov 2013; published 21 Nov 2013

and unwanted nonlinear loss processes in cladding-pumped fiber lasers, and allow scaling to higher output power has resulted in the development of a number of different schemes to achieve preferential lasing on the fundamental mode. For example the use of distributed mode filtering through bend loss [4] or specially designed microstructured fibers [5]. By contrast, somewhat less effort has been devoted towards selection of individual high-order transverse modes in spite of the potential benefits to performance, which include higher threshold for detrimental nonlinear loss processes [6], reduced sensitivity to mode skew [7] as well as the potential for improved energy extraction in pulsed systems. Techniques for selecting higher order modes in multimode fiber oscillators are often quite difficult to implement and lack the flexibility to switch between modes to suit the application. It has been shown that in some laser processing applications the desired beam profile and polarization behavior is dictated by the type of material being processed [8,9]. Indeed, independent of polarization the use of donut-shaped beams or beams with dynamically adaptable transverse profiles could yield substantially higher processing speeds as well as improved cut quality in a range of materials processing applications [10,11].

In this paper we present a simple technique to allow the electronically controllable selection of individual transverse modes within a multi-mode fiber laser oscillator. We exploit the different spectral responses of in-fiber Bragg gratings (FBGs) and free space wavelength selective elements to simultaneously achieve wavelength selection and spatial mode selection in a simple fiber laser with an external feedback cavity architecture [12]. By using an electronically addressable acousto-optic tunable-filter (AOTF) in place of a mechanical tuning element we are now able to select the oscillating mode without the need for mechanical movement, allowing fast switching of transverse modes within the oscillator. This approach has been applied to a core-pumped multimode Tm-doped silica fiber laser to selectively excite the fundamental mode (LP_{01}) and next higher order mode (LP_{11}) at power levels in excess of 5W by simply adjusting the RF drive frequency to the AOTF. Fast switching between LP_{01} and LP_{11} mode at ~kHz repetition rates was also realized.

2. Principle of operation

Through periodic spatial modulation of a material's refractive index, Bragg gratings allow narrow band reflection of optical signals with a high efficiency and reflectivity. For a given wavelength, the Bragg condition is given by:

$$\lambda = 2n\Lambda\cos(\theta) \tag{1}$$

where θ is the angle of incidence of the incoming signal with respect to the grating normal, n is the mean refractive index of the medium and Λ is the period. Volume Bragg gratings (VBGs) and acousto-optic tunable-filters (AOTFs) are common examples of robust free space Bragg selective elements. Volume Bragg gratings, where a fixed Bragg period is written into photo-thermo refractive (PTR) glass have a fixed resonance wavelength when operated at normal incidence. However by changing the angle of incidence θ the resonance wavelength of the VBG can be down tuned to shorter wavelengths allowing narrowband wavelength tuning [13]. In the case of an acousto-optic device such as an AOTF the Bragg period is no longer fixed by photo-inscription, but rather defined by the period of an incident acoustic wave driven by an input RF signal. By changing the RF drive frequency, and hence acoustic wavelength, the resonance wavelength of the AOTF can also be shifted. A unique property of the AOTF is the static position of deflected beam independent of the grating period (RF drive frequency). This allows an AOTF to be used as a wavelength-tunable element without any need for physical movement of the optical system.

For the special case of Bragg gratings written into waveguides, the effect of mode propagation on the Bragg resonance wavelength must be taken into account. Bragg resonance within a waveguide is dependent on the effective index of the guided modes rather than a mean index of the medium. For in-waveguide gratings the Bragg condition is given by:

#196993 - $15.00 USD Received 10 Sep 2013; revised 2 Nov 2013; accepted 5 Nov 2013; published 21 Nov 2013

$$\lambda_{FBG} = 2n_{eff}\Lambda_{FBG} \quad (2)$$

where, Λ_{FBG} is the grating period within the waveguide, n_{eff} is the effective index of the guided mode and λ_{FBG} is the wavelength at which resonance occurs. The propagation constant and associated effective index n_{eff} of guided modes within a step index waveguide is governed by the core and cladding refractive indices as well as the modal order, where $n_{core} > n_{eff} > n_{clad}$. The fundamental mode has an effective index closest to that of the core, with higher order modes having progressively lower effective indices until the condition for guidance is no longer met. Thus, for a Bragg grating written into a multi-mode waveguide the Bragg condition for each mode is satisfied at different wavelengths. Hence, higher order modes propagating with a lower effective index to that of the fundamental mode see resonance at shorter wavelengths. This phenomenon is seen as a multi peak behavior in both the transmission and reflection spectrum of multi-mode FBGs [14]. By forming a laser cavity consisting of a highly reflecting FBG written into the core of a multimode active fiber and an external cavity free space wavelength-selective element, we can exploit the different spectral responses of the two elements to selectively excite individual transverse modes within the oscillator [12]. Moreover, by employing an AOTF as the free-space wavelength-selective element it is now possible to electronically select and switch between different transverse modes by changing the RF drive frequency without the need for mechanical adjustment and realignment of the external cavity.

3. Experimental layout and results

The laser cavity design used in our experiments (shown in Fig. 1) comprised of a 30cm length of multimode thulium-doped fiber with feedback for lasing provided by a Bragg grating written directly into the core of the active fiber at one end, and at the opposite end by an external feedback cavity. The latter contained an AOTF and a broadband reflector (HR) to provide the required wavelength-dependent feedback. A half-wave plate was also placed in the external cavity between the AOTF and fiber collimating lens to allow polarization direction to be aligned for optimum diffraction efficiency in the AOTF. Broadband feedback via Fresnel reflection at the fiber end adjacent to the external cavity was suppressed with a 14° angle cleaved facet. The active fiber used in our experiments was fabricated in-house and had a 18μm diameter (0.22 NA) aluminosilicate core co-doped with 1 wt% thulium concentration. The corresponding V-number was 6.3, hence the core could guide ~6 LP modes. In order to increase the photosensitivity of the fiber core, germanium was also added as a co-dopant during the MCVD fabrication process and hydrogen loading was performed before FBG inscription. The fiber had a non-circular outer-cladding as it was originally designed for used in a cladding-pumped laser architecture. As a result, the fiber core became slightly elliptical during the fiber drawing process with a ratio of the core's major-to-minor axis of ~1.1. Pump light was provided by a commercially available 20W single-mode 1565nm Er,Yb fiber laser source and was coupled into the doped fiber with the aid of wavelength division multiplexer (WDM) and a short length of single mode passive fiber (Nufern SM1950) spliced directly to the active fiber adjacent to the FBG. The FBG had an estimated reflectivity of >80% for the fundamental mode and bandwidth of 0.2nm (FWHM) with Bragg resonance for the fundamental mode at 1925.5nm under unpumped conditions. The AOTF used in our experiment was supplied by Gooch & Housego and could be operated over the entire 1700-2100nm Tm emission band. The single-pass bandwidth of the AOTF was 2nm (FWHM) at 2000nm and the single-pass diffraction efficiency could be varied from 0 to 70% for a linearly-polarized input by simply adjusting the RF drive power. Laser output was taken from the zeroth-order beam of the AOTF.

#196993 - $15.00 USD Received 10 Sep 2013; revised 2 Nov 2013; accepted 5 Nov 2013; published 21 Nov 2013

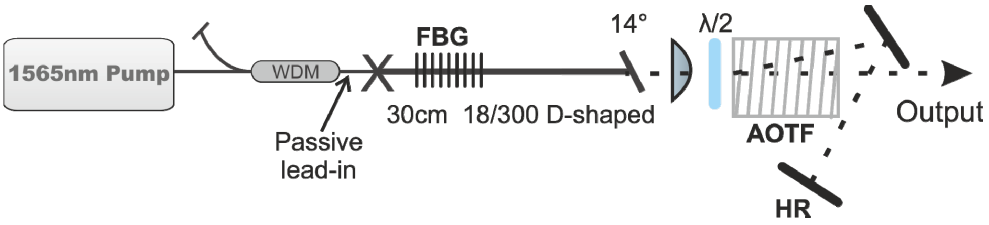

Fig. 1. Experimental layout of cladding-pumped Tm-doped fiber laser.

Using an arbitrary function generator (Tektronix AWG3102) the RF drive frequency of the AOTF was adjusted to allow the operating wavelength to be tuned across the Bragg resonance peaks of the multi-mode FBG. In CW mode of operation the fundamental or next higher order modes could be selected. Figure 2(a) shows the selection of the fundamental mode, with selection of the donut-shaped (incoherent superposition of LP_{11}) modes shown in Fig. 2(b). Due to the limited wavelength resolution of the AOTF and FBG, and close effective index spacing (and hence wavelength spacing) of still higher order modes within this fiber, it was not possible to excite these modes individually. The resonance wavelength of the FBG was found to be pump power dependent with ~4pm/W shift to longer wavelengths. The latter was attributed to quantum defect heating in the fiber core. At a launched pump power of 17W the fundamental mode resonance was 1926.2nm, whilst the next guided modes corresponding to the LP_{11} group of modes were found to lase at 1922nm.

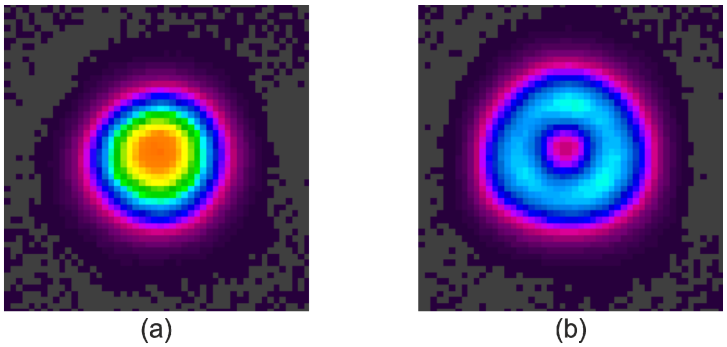

Fig. 2. Output beam profile for AOTF tuned to (a) LP_{01} mode and (b) LP_{11} mode superposition.

The maximum CW output powers for the LP_{01} mode and a donut-shaped LP_{11} superposition were 5.8W and 5.1W respectively (see Fig. 3). Additionally, the emitted modes demonstrated a linear polarization perpendicular to the optical bench, with the LP_{11} superposition demonstrating a polarization extinction ratio (PER) of ~10dB, whilst the fundamental mode had a PER of >20dB. The beam propagation factors (M^2) for the fundamental mode and LP_{11} superposition were measured to be 1.07 and 2.23 respectively, in close agreement with theory.

#196993 - $15.00 USD Received 10 Sep 2013; revised 2 Nov 2013; accepted 5 Nov 2013; published 21 Nov 2013

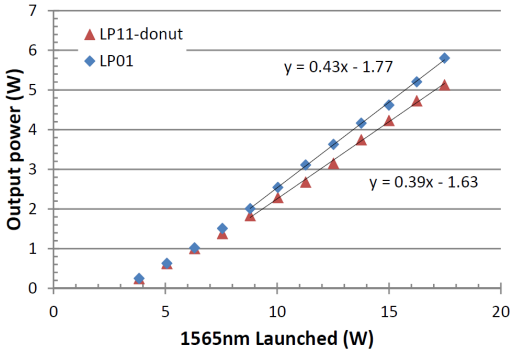

Fig. 3. Laser output power for LP_{01} (blue) and $LP_{11\text{-donut}}$ (red) modes.

When tuned to the LP_{11} donut mode the laser emission spectrum was found to comprise of two peaks of roughly equal power separated by ~0.2nm. Any misalignment of the feedback mirror in the plane of incidence (or in the orthogonal direction) resulted in a reduction in power for one of the emission wavelengths and a noticeable two-lobe intensity profile associated with preferential lasing on a particular LP_{11} mode orientation. This observation is consistent with our assertion that the donut mode is an incoherent superposition of orthogonally orientated non-degenerate vector modes rather than a circularly symmetric vector mode.

Further detailed analysis of the allowed modes for this fiber using commercial mode solving software shows that the normally degenerate vector modes making up the LP_{11} separate into two degenerate groups with two lobed profiles and is caused by the slightly elliptical nature of the core. As a consequence, the generation of azimuthally symmetric vector modes is excluded in this type of fiber [15]. Further experimental confirmation of the above explanation for donut-mode generation was obtained by inserting a solid etalon of 0.5mm thickness (2.5nm free-spectral-range) and double-pass bandwidth of 0.05nm (FWHM) into the external feedback cavity between the AOTF and HR mirror. This was used to enhance wavelength discrimination within the feedback cavity and allow the individual peaks of the LP_{11} mode group to be resolved. With the AOTF tuned to the LP_{11} peak, the solid etalon was angle tuned to match either wavelength peak of the dual peak output. The results (illustrated in Fig. 4) confirm that the two lobe output profile orientation was dependent on the resonance wavelength. The two lobe orientation changed by 90 degrees when etalon transmission peak, and hence lasing wavelength, is adjusted from the 1921.7nm peak to the 1921.9nm peak in agreement with our theoretical model.

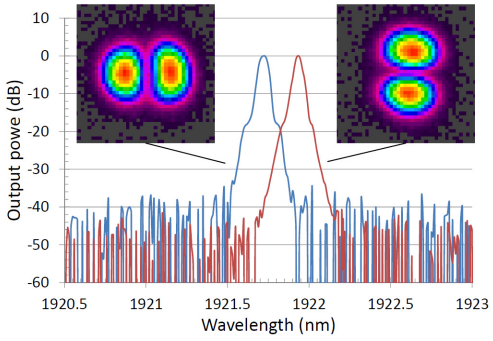

Fig. 4. Output spectrum and corresponding beam profiles when tuned to the LP_{11} mode group with solid etalon used for fine wavelength selection.

#196993 - $15.00 USD Received 10 Sep 2013; revised 2 Nov 2013; accepted 5 Nov 2013; published 21 Nov 2013

By switching the resonance wavelength of the external cavity between resonance for the fundamental mode and resonance for the donut-shaped superposition of modes we could switch rapidly between the two mode shapes. This rather useful feature of laser behavior is made possible by the ability to rapidly switch between resonance wavelengths in an AOTF. With the appropriate fiber, FBG and AOTF designs could be extended to a wider range of transverse modes. To investigate the limits on the switching behavior in our present laser, the feedback wavelength for the AOTF was switched between LP_{01} and LP_{11} lasing wavelengths at repetition rates ranging from ~Hz to > 10kHz. The laser output profile was monitored using a pyroelectric array camera (Pyrocam III). For repetition rates up to 8Hz the Pyrocam allowed direct observation of complete switching between the LP_{01} and LP_{11} modes, a recording of which can be found in Media 1. Direct observation of laser switching behavior was not possible at higher repetition rates due to the limited frame rate of 48Hz for the pyroelectric array. To investigate switching behavior at higher frequencies, a volume Bragg grating with a 0.5nm reflection bandwidth was used to discriminate between the different lasing wavelengths and hence allow direct measurement of the relative modal intensities. The laser switching behavior for repetition rates up to 40kHz was investigated. At low frequencies the output profile of the laser was simply that of equal parts LP_{01} and LP_{11} donut. Whilst at higher switching frequencies the LP_{01} mode tended to dominate the laser output. Adjustment of the relative RF drive powers on the AOTF, and hence the relative optical feedback efficiencies for the two modes, allowed this effect to be mitigated resulting in equal excitation of the fundamental and donut shaped mode at up repetition rates of 20kHz. For switching frequencies above this rate the limited build-up time for the AOTF wavelength selection resulted in too short a feedback duration for stable lasing to occur. Figure 5 shows the time profiles for 1kHz, 10kHz and 20kHz switching rates.

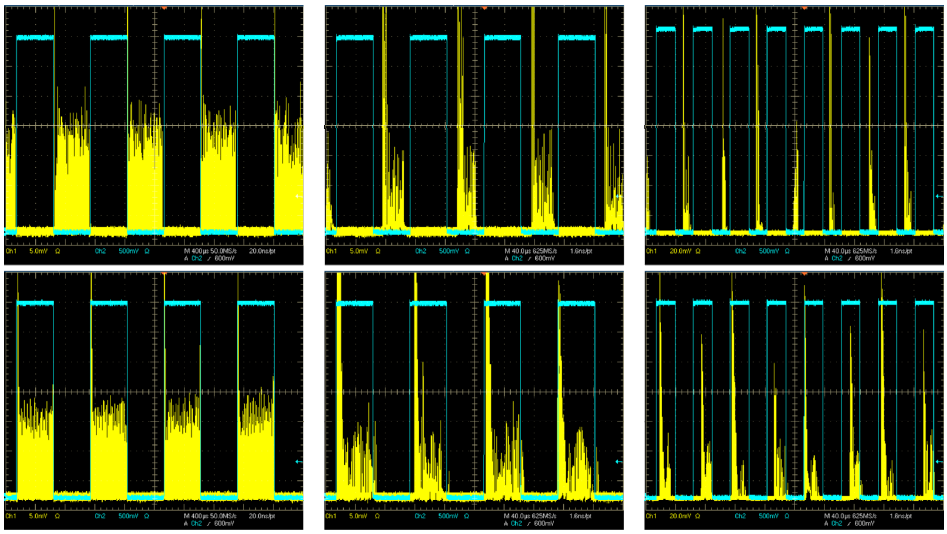

(a) 1kHz (400µs/dev) (b) 10kHz (40µs/dev) (c) 20kHz (40µs/dev)

Fig. 5. Laser output time profiles for mode switching speeds of (a) 1kHz, (b) 10kHz and (c) 20kHz. A volume Bragg grating was used to spectrally separate the output of the two modes with top row showing the $LP_{11\text{-donut}}$ component of the laser output and bottom row showing LP_{01} component.

The wavelength selectivity of the AOTF used in these experiments was less than that required to cleanly excite the individual two lobed modes of the LP_{11} peak. However by inserting an appropriately spaced Fabry–Pérot filter into the external feedback cavity along with the AOTF it is possible to switch between either one of the two orthogonally orientated

#196993 - $15.00 USD Received 10 Sep 2013; revised 2 Nov 2013; accepted 5 Nov 2013; published 21 Nov 2013

LP_{11} mode groups and the fundamental LP_{01} mode whilst still maintaining the electronic control of the AOTF arrangement. Here the free spectral range of a Fabry–Pérot filter is chosen to match the wavelength spacing between the LP_{01} and either of the two LP_{11} peaks. This was experimentally realized by the construction of a variable separation Fabry–Pérot wavelength filter, consisting of two 90% reflective plane mirrors. One mirror was placed on a mechanical translation stage allowing course adjustment of mirror separation, with fine adjustment achieved by piezoelectric positioner. For a mirror separation of ~430μm the resulting free spectral range and double-pass spectral selectivity of 4.3nm and 0.07nm were achieved, allowing the long wavelength 1921.9nm LP_{11} peak and 1926.2nm LP_{01} peak to be selected and switched (Media 2). By decreasing the mirror separation of the Fabry–Pérot filter to 410μm it was possible to select between the short wavelength 1921.7nm LP_{11} peak and the fundamental mode.

4. Conclusion

We have demonstrated for the first time, to the best of our knowledge, the rapid selection and switching between transverse modes in a multimode fiber laser oscillator using a novel electronically controllable mode selection technique. This technique is also scalable to both pulsed configurations and high average output powers. With this simple arrangement we were able to generate greater than 5W of output power in the fundamental or next higher order mode, and demonstrate the control and switching between modes at repetition frequencies up 20kHz. By using a combination of both active and passive wavelength selective components we have further enhanced the external cavity wavelength selectivity, circumventing the resolution limitations of the AOTF whilst still allowing active selection and switching between modes. This technique allows a new level of flexibility in transverse mode control in multimode fiber laser enabling dynamic control of modal content to suit advanced laser processing applications.

Acknowledgments

This work was funded by the EPSRC Centre for Innovative Manufacturing in Photonics (EP/H02607X/1) and by the European Commission under the Seventh Framework programme (HALO project no. 314410).

#196993 - $15.00 USD Received 10 Sep 2013; revised 2 Nov 2013; accepted 5 Nov 2013; published 21 Nov 2013